

Aerodynamic Analysis of a Symmetric Aerofoil

Narayan U Rathod

Department of Mechanical Engineering, BMS college of Engineering, Bangalore, India

Abstract - The main parameters deciding the performance of an aerofoil are geometry, Reynolds number and co-efficient of lift. The project carried out to emphasize mainly the parameters such as the distribution of pressure and velocity over a symmetrical aerofoil surface and to obtain the characteristic curves. The experimental approach has been applied to carry out the parametric study and results are being validated with the established results.

Index Terms - Aerodynamic analysis, lift curve, Pressure Distribution, Symmetric aerofoil, Velocity Distribution

NOMENCLATURE

α = angle of attack
 C_p = coefficient of pressure
 C_D = coefficient of drag
 C_L = coefficient of lift
 $U.P = P_u$ = pressure on upper surface
 $L.P = P_L$ = pressure on lower surface
 $U.V = V_u$ = velocity on upper surface
 $L.V = V_L$ = velocity on lower surface
 V_∞ = free stream velocity
 P_∞ = free static pressure
 Re = Reynolds number
 ρ = Density
 c = Chord
 S = planform area

I. INTRODUCTION

A wing is a three-dimensional shapes that, when immersed in an appropriate flow, will produce usable force from a pressure imbalance. An aerofoil is the shape of a wing or blade or sail as seen in cross-section.

An aerofoil-shaped body moved through a fluid produces an aerodynamic force. The component of this force perpendicular to the direction of motion is called lift. The component parallel to the direction of motion is called drag.

II. AERO FOIL NOMENCLATURE

The various terms associated with an aerofoil are as follows:

1. **Leading edge:** It is the forward end of the aerofoil that faces the free stream during flight.
2. **Trailing edge:** It is the rearward end of the aerofoil.
3. **Mean camber line:** It is the locus of the point's midway between the upper and the lower surfaces measured perpendicular to the mean camber line itself.
4. **Chord line:** It is a straight line connecting the leading and the trailing edges. The precise distance between the leading and the trailing edges is termed as 'chord'.
5. **Camber:** It is the maximum distance between the chord line and the mean camber line measured perpendicular to the chord line. A symmetric aerofoil is one with zero camber
6. **Thickness:** It is the distance between the upper and the lower surfaces measured perpendicular to the chord line

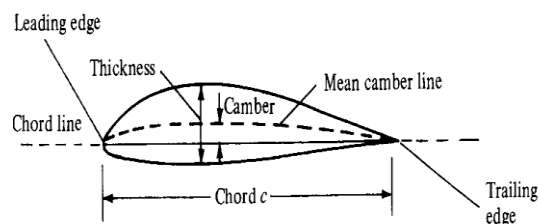


Fig.1 Characteristics of an aerofoil

The NACA aerofoils are classified into various series based on the number of digits that define the aerofoil configuration. The 4 digit series which is used in this project is explained below.

NACA Four Digit Series: In this series four digits are used to define the geometry of the aerofoil. The significance of the four digits are as follows,

First figure-The maximum camber as a percentage of chord.

Second figure-The position of maximum camber in tenths of chord.

Third and fourth figure-The maximum thickness as a percentage of chord.

Example: the profile NACA 4412 has a maximum camber of 4% at 40% of the chord, and a maximum thickness of 12%.

III. AERODYNAMIC FORCES AND MOMENTS

A wing is a three-dimensional shapes that, when immersed in an appropriate flow, will produce usable force from a pressure imbalance. Pressure on the upper surfaces of the wing of an aircraft is usually lower and on the lower surface it is higher. This difference in pressure between the two surfaces provides the necessary lift force which keeps the aircraft afloat during flight.

In the simplest form of motion of an aircraft, i.e., straight and level unaccelerated flight, equilibrium is maintained between the weight and lift force and engine thrust and drag force.

The description of various forces is as follows-

- 1) Lift- It is the force that acts upwards perpendicular to the direction of flight or free stream.
- 2) Drag- It is the force that acts in the opposite direction to the line of flight and resists the motion of the aircraft.
- 3) Centre of Pressure-It is the point on the aerofoil at which the resultant aerodynamic force acts.
- 4) Pitching Moment- It is the moments which acts in the plane containing drag and lift forces and is considered positive when it tends to raise the aircraft nose.
- 5) Aerodynamic Centre- It is that point about which pitching moment is independent of angle of attack.
- 6) Lift Coefficient- Lift coefficient may be defined as the ratio of lift pressure to dynamic pressure, where as lift pressure is the ratio of lift to reference area. The lift coefficient may be used to relate the total lift generated by a foil equipped craft to the total area of the aerofoil.

$$C_L = \frac{L}{\frac{1}{2}\rho v^2 S} = \frac{2L}{\rho v^2 S} = \frac{L}{qS}$$

- 7) Drag Coefficient: It is a dimensionless parameter used to quantify the amount of drag exerted by a body.

$$C_d = \frac{2F_d}{\rho v^2 A}$$

IV. AEROFOIL SPECIFICATIONS

In order to understand the analysis of the various parameters of the aerofoil, the NACA 0017 aerofoil was selected and experiments were conducted by using a low speed wind tunnel. For a symmetric aerofoil, no lift is generated at zero incidence (i.e. $C_l = 0$ at 0° angle of attack). Considering the wind tunnel specification constraints, the aerofoil dimensions of chord $C = 30$ cm (approximately 1/3 rd of the test section length to provide a uniform stream line air flow), maximum thickness of $t = 5.1$ cm (corresponding to NACA 0017 series) and width of 20 cm with 11 pressure tapping holes was selected. These parameters were selected also keeping in mind that in general, the aerofoil cross section should be less than 2% of the test section cross section.

Table-1. Pressure tapping specifications

Pressure tapping number	Distance from leading edge
1	2.8
2	4.7
3	5.8
4	7.8
5	8.6
6	11.5
7	13.8
8	15.6
9	18
10	21.1
11	23.2

V. SETUP DETAILS

A suitable mechanism was designed and fabricated to hold the aerofoil and facilitate the change in angle of attack. The concept of a slotted lever was utilized to provide 2 degrees of freedom i.e. both translation along y direction and rotation about the pivot was provided. A reference protractor on one of the test section sides was used for setting and measurements of angle of attack.

An inclined multi-tube manometer with a range of 0-160 mm WG was used to measure the pressure values in the 11 pressure tapping's over the aerofoil surface.

A low speed Blower type wind tunnel was used for experimentation capable of generating a free stream air velocity of up to 45 m/s.

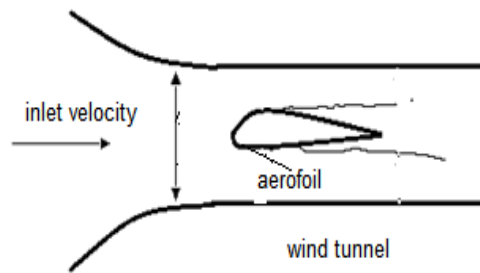


Fig. 2 wind tunnel setup

VI. METHODOLOGY

The free stream velocities and stagnation pressures at different blower rotational speeds by using pitot static manometer were determined. The aerofoil mechanism was assembled and the angle of attack was set to zero degrees. The pressure tapping tubes from the aerofoil were connected to the multi-tube manometer in sequence and the pressure values for both the upper and lower surfaces were determined after the setup was allowed to reach the steady state conditions.

The above procedure was repeated to determine the pressure values at different blower rotational speeds and at different angles of attack.

COEFFICIENT OF PRESSURE

The coefficient of pressure is calculated for both the upper and lower surfaces by measuring the water head in the multi tube manometer.

Pressure at a point in the aerofoil is given by:

$$P = \rho_{water} g \Delta H_{water} \tag{1}$$

From Bernoulli's equation,

$$P + \frac{1}{2} \rho V^2 = P_{\infty} + \frac{1}{2} \rho V_{\infty}^2 \tag{2}$$

By knowing the free stream values of pressure and velocity and the pressure on the aerofoil surface, the velocity of air at the aerofoil surface is determined using Eq. 2.

The coefficient of pressure is calculated by the equation

$$C_p = \frac{P - P_{\infty}}{\frac{1}{2} \rho U_{\infty}^2} \tag{3}$$

The values of coefficient of pressure are computed for different blower speeds and different angles of attack for both the upper and lower surfaces.

COEFFICIENT OF LIFT

Pressure is a stress, i.e., it is a force per unit area. In order to determine the actual force produced by a stress, we must sum all the pressure contributions over the entire surface, thus we must integrate the pressure over the surface, If we split the airfoil surface into upper and lower parts, we can write the coefficient of lift for the airfoil as

$$C_L = \frac{1}{c} \int_{LE}^{TE} C_{pl} - \frac{1}{c} \int_{LE}^{TE} C_{pu} dx = \frac{1}{c} \int_{LE}^{TE} (C_{pl} - C_{pu}) dx \tag{4}$$

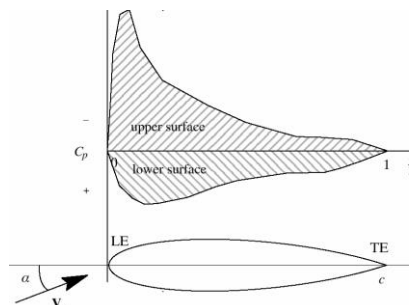


Fig. 4. Distribution of C_p over aerofoil surface

In these expressions, x is the coordinate along the chord line and c is the length of the chord, i.e. the length from the LE to the TE , so we can define a dimensionless variable x/c that varies from 0 at the leading edge LE , to 1 at the trailing edge TE . Because c is a constant, we can move it inside the integral and write the C_l equation in terms of the fraction of the chord x/c

$$C_L = \int_0^1 (C_{pu} - C_{pl}) d\left(\frac{x}{c}\right) \quad (5)$$

Evaluated on the lower surface and upper surface, integrated along the chord line in terms of the fractional distance measured from the leading edge to the trailing edge. The integral in above equation represents the cross hatched area between the C_{pu} and C_{pl} curves. Since the C_p values are determined experimentally, we resort to a numerical method for actually computing the integral in the above equation. We use one of the simplest numerical methods for computing integrals, the trapezoidal rule to evaluate the values of C_L for different angles of attack using Eq.5.

VII. RESULTS AND DISCUSSION

From the values obtained experimentally, the pressure and velocity distributions are plotted. These represent the changes in the parameters over the aerofoil surface. The following graphs are plotted that illustrate the effect of distribution of pressure and velocity over the aerofoil surface for different angle of attack on the NACA 0017 series aerofoil.

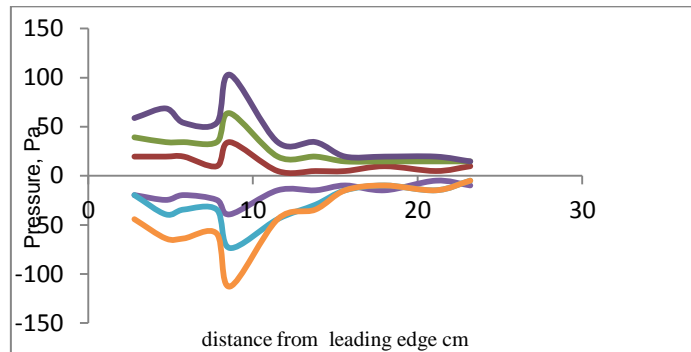


Fig. 5 Pressure distribution at 0° angle of attack

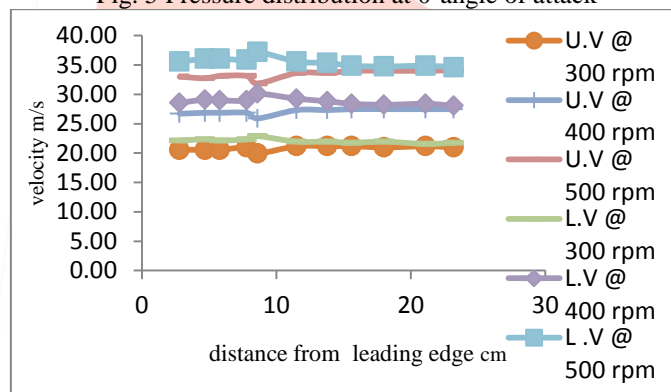


Fig. 6 Velocity distribution at 0° angle of attack

From the graph, it can be seen that the pressure distribution on both upper and lower surfaces are similar, suggesting no lift generation. The velocity curves flatten near the trailing edge.

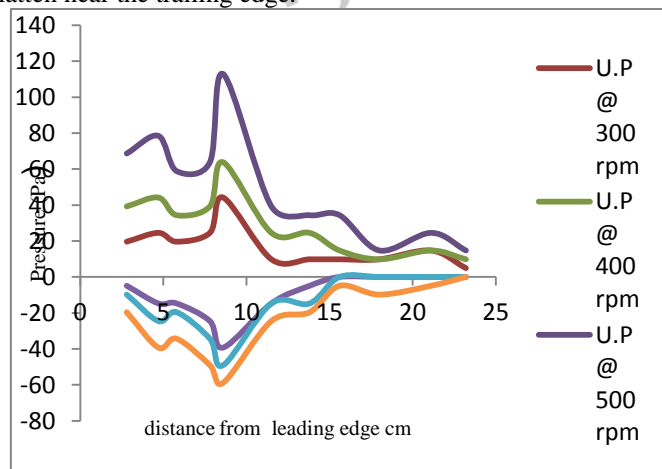


Fig. 7 Pressure distribution at 2° angle of attack

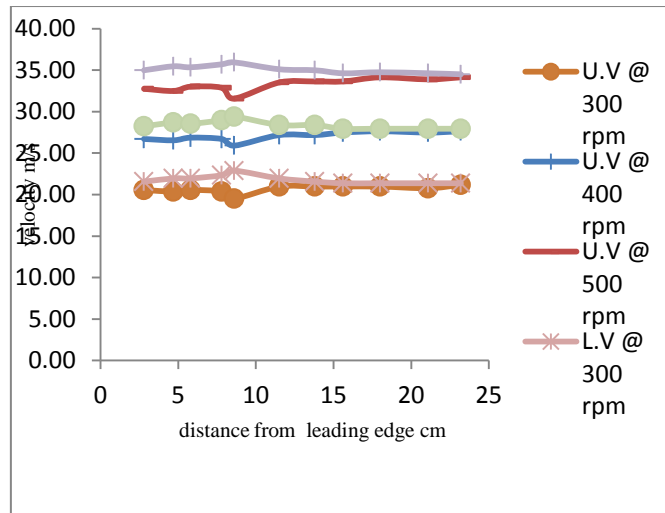


Fig. 8 Velocity distribution at 2⁰ angle of attack

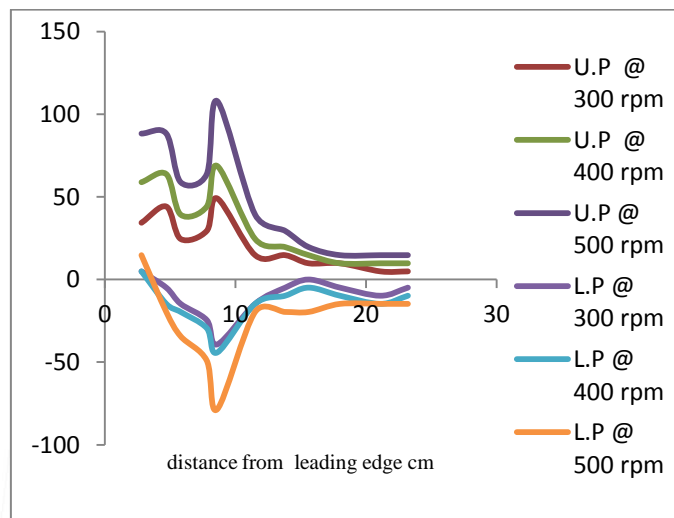


Fig. 9 Pressure distribution at 4⁰ angle of attack

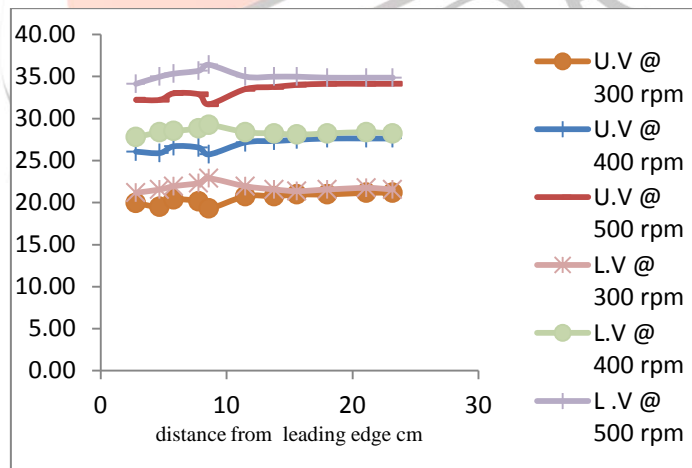


Fig.10 Velocity distribution at 4⁰ angle of attack

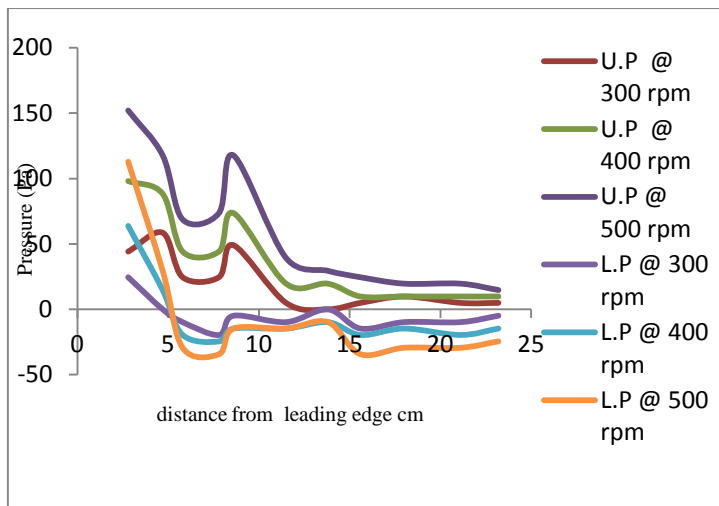


Fig.11 Pressure distribution at 8° angle of attack

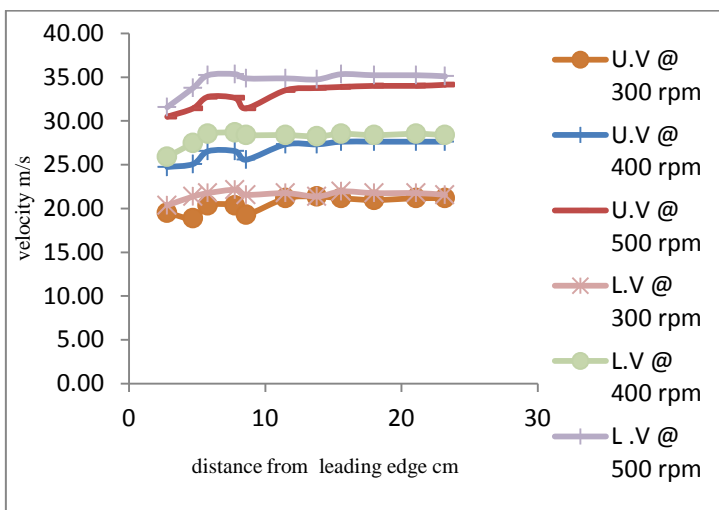


Fig.12 Velocity distribution at 8° angle of attack

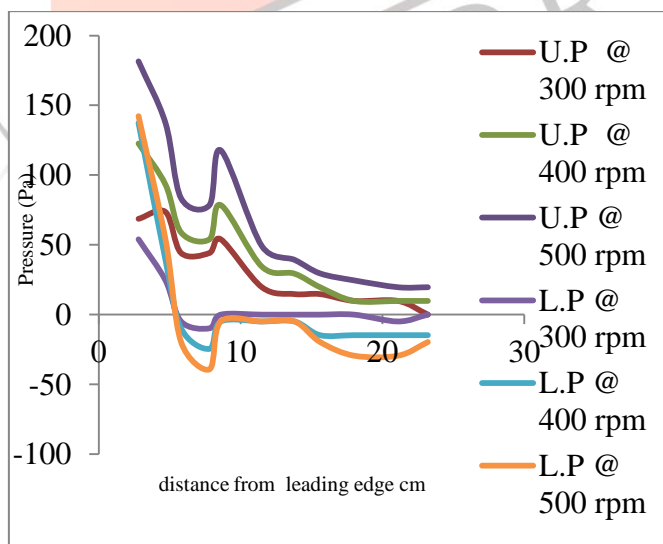


Fig. 13 Pressure distribution at 12° angle of attack

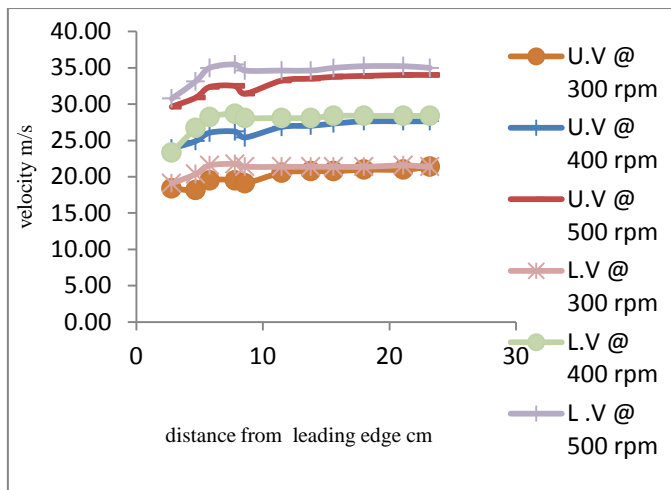


Fig.14 Velocity distribution at 12° angle of attack

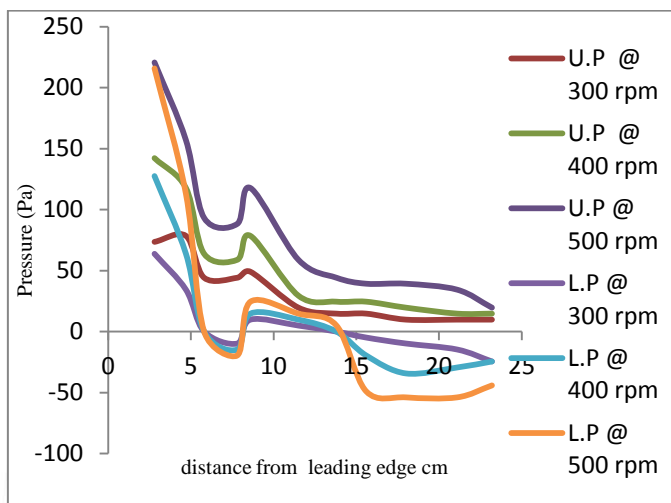


Fig. 15 Pressure distribution at 14° angle of attack

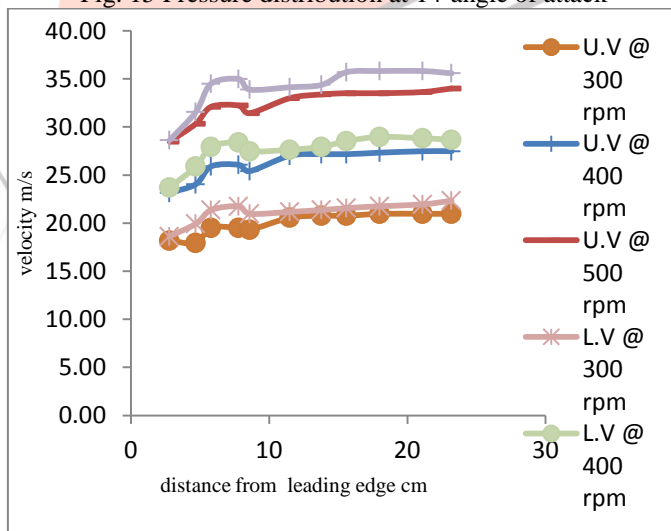


Fig.16 Velocity distribution at 14° angle of attack

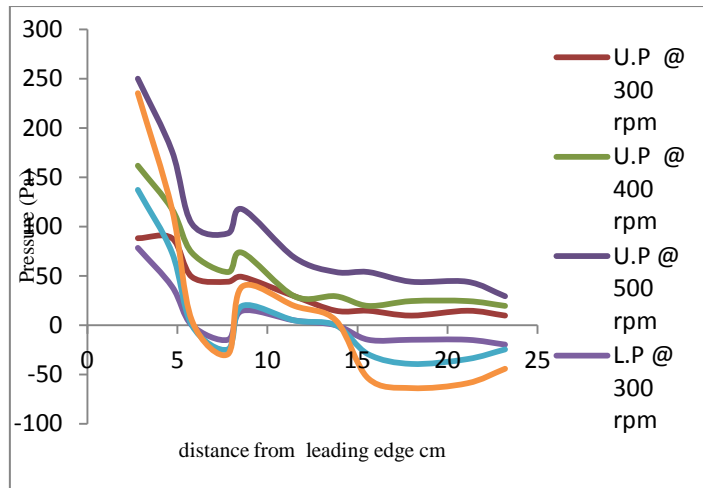


Fig. 17 Pressure distribution at 16° angle of attack

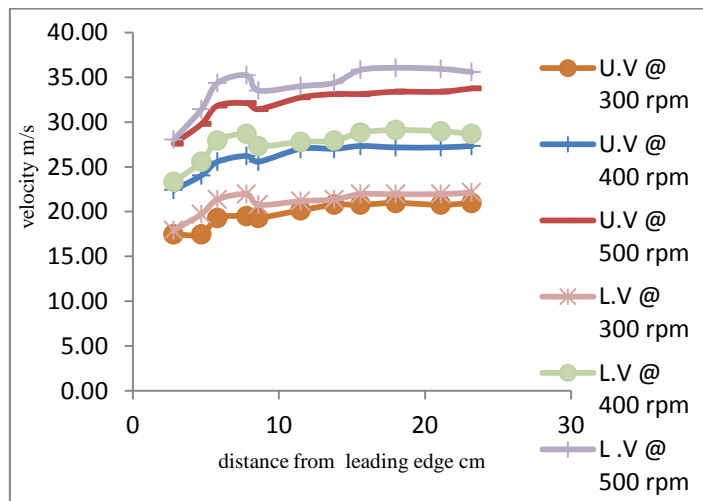


Fig.18 Velocity distribution at 16° angle of attack

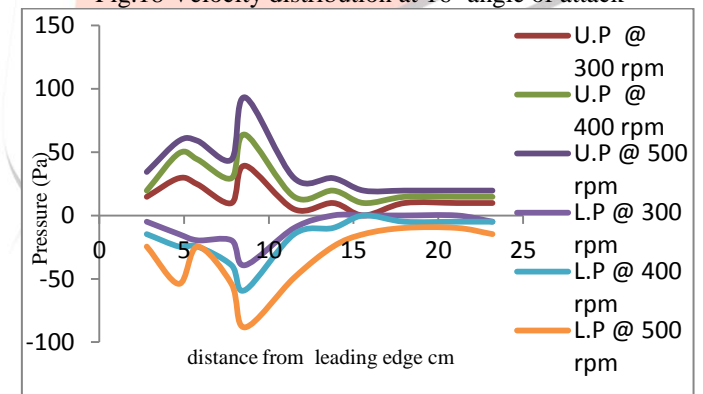


Fig. 19 Pressure distribution at -2° angle of attack

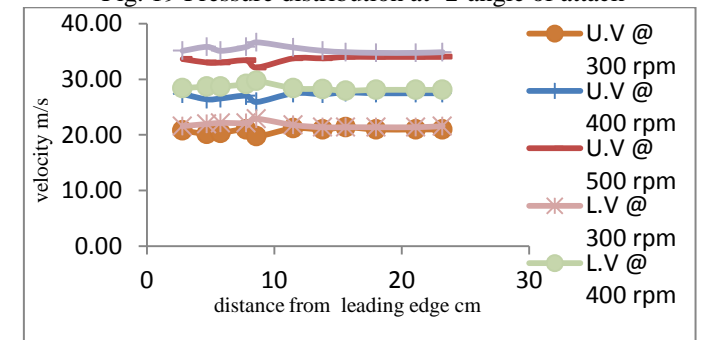


Fig.20 Velocity distribution at -2° angle of attack

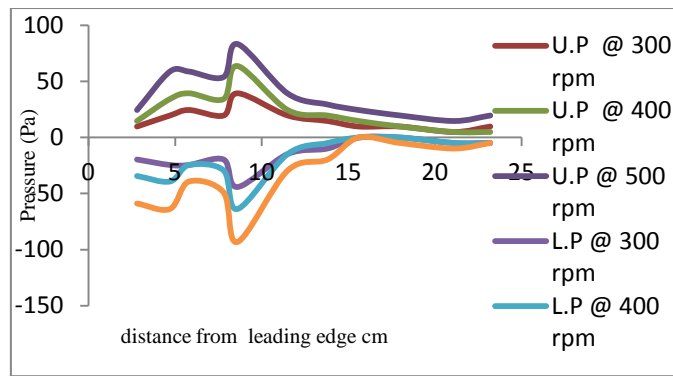


Fig.21 Pressure distribution at -4° angle of attack

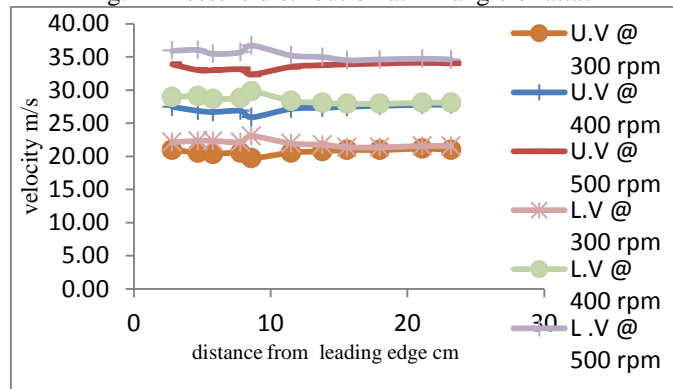


Fig.22 Velocity distribution at -4° angle of attack

The following inferences can be drawn from the velocity and pressure distribution graphs:

At zero angle of attack the pressure distribution over the upper surface is similar to the pressure distribution on the lower surface, this implies that no lift is generated at Zero degrees.

The pressure and velocity values increase with the increase in speed of the blower.

From the pressure variation graphs it can be concluded that the flat region of the curve near the trailing edge signifies that the flow separation has occurred.

It can be concluded that the pressure in the separated region remains constant and is independent of Reynolds number. Whereas the pressures over the remainder of the upper surface decrease with the increasing Reynolds number.

Characteristic Lift Curves:

The characteristic curves obtained are at different angles of attack are as follows:

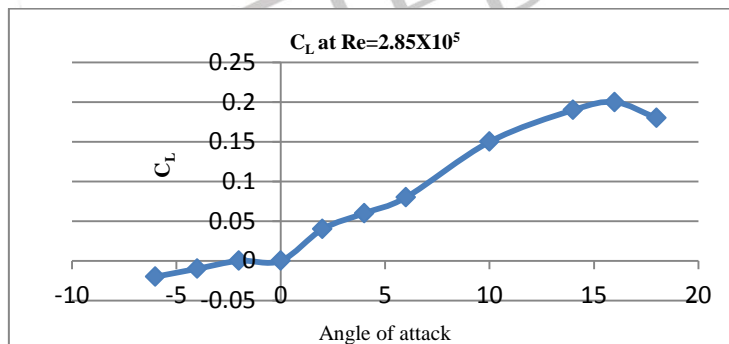


Fig.23 characteristic lift curve at $Re=2.85 \times 10^5$

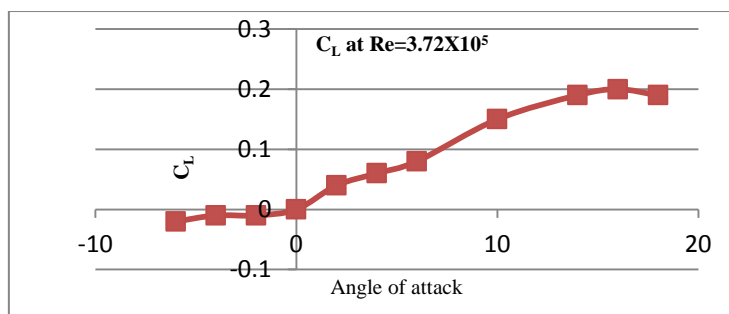


Fig.25 characteristic lift curve at $Re=3.72 \times 10^5$

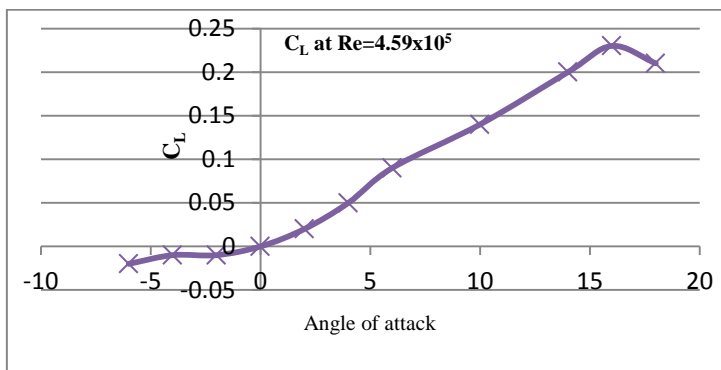


Fig.26 characteristic lift curve at $Re=4.59 \times 10^5$

The graph below shows the variation of the co-efficient of lift with the angle of attack conducted by NACA at L.M.A.L. at similar conditions of flight ($V = 21$ m/s).

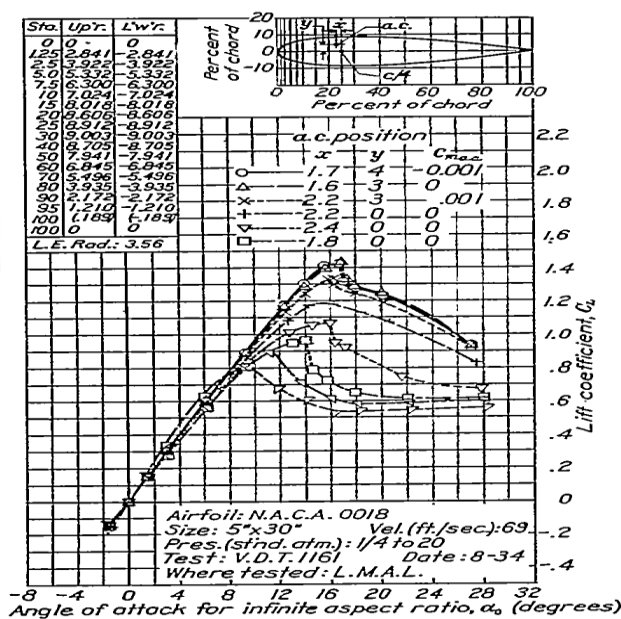


Fig.27 Report number 586 NACA

Comparing Fig.24 and Fig.27, it can be concluded that the characteristic graphs so obtained by experiments are in good agreement with the well established graphs obtained from theoretical approach.

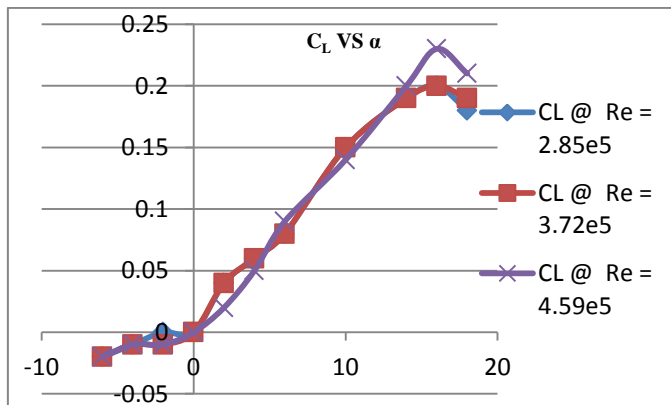


Fig.28 Variation of C_L with α

From the characteristic graphs obtained through experiments the average stalling angle was found to be approximately equal to 16° .

INFERENCES

From the characteristic graphs it can be seen that the slope of the curve decreases with the increase in Reynolds number.

From the pressure variation graphs, it can be concluded that the flat region of the curve near the trailing edge signifies that the flow separation has occurred. It can be concluded that the pressure in the separated region remains constant and is independent of Reynolds number. Whereas the pressures over the remainder of the upper surface decrease with the increasing Reynolds number.

The increase in the lift of the section with the increase in Reynolds number is seen to be connected directly with the decrease of pressure on the upper surface and the increase in the pressure on the lower surface.

It can be seen that C_L increases linearly with α , until an angle of attack is reached where the wing stalls. C_L reaches a peak value and the decreases with further increase in α . This maximum value of C_L is denoted as $C_{L\max}$.

For a given airplane flying at a given altitude, W , ρ and S are fixed values; hence from the equation below, each value of velocity corresponds to a specific value of C_L . In particular V_∞ will be smallest when C_L is maximum. Hence, the stalling velocity for a given airplane is determined by $C_{L\max}$ from the equation below.

$$V_\infty = \sqrt{\frac{2W}{\rho_\infty S C_L}}$$

REFERENCES

- [1] John D. Anderson, *Fundamentals Of Aerodynamics*, Tata McGraw Hill publications, 2nd edition
- [2] E. Lo Houghton and PW Carpenter, *Aerodynamics For Engineering Students*, 5th edition, Butterworth-Heinemann
- [3] Daniel P Raymer, *Aircraft Design: A Conceptual Approach*, 5th edition, AIAA Education Series
- [4] E. N. Jacobs, K. E. Ward, & R. M. Pinkerton, "THE CHARACTERISTICS OF 78 RELATED AIRFOIL SECTIONS FROM TESTS IN THE VARIABLE-DENSITY WIND TUNNEL", 1933, NACA report number 460
- [5] Eastman N. Jacobs and Albert Sherman, "AIRFOIL SECTION CHARACTERISTICS AS AFFECTED BY VARIATIONS OF THE REYNOLD'S NUMBER" NACA report number 586
- [6] Darrol Stinton, *the Design of the Aeroplane*. Bsp Professional Books (October 1985)

